The Wyville Thomson Ridge Complex located in the NE Atlantic – aspects of the tertiary development

Nielsen, Ingun Ziska; Boldreel, Lars Ole

Published in:
Faroe Islands Exploration Conference

Publication date:
2012

Document version
Publisher's PDF, also known as Version of record

Ritchie, J.D., Johnson, H. and Kimbell, G.S. 2003. The nature and age of Cenozoic contractional deformation within the NE Faroe-Shetland Basin. *Marine and Petroleum Geology*, 20, 399-409.

Ritchie, J.D., Johnson, H., Quinn, M.F., and Gatliff, R.W. 2008. The effects of Cenozoic compression and the Cenozoic Faroe-Shetland Basin and adjacent areas. In: Johnson, H., Dore, T.G., Gatliff, R.W., Holdsworth, R.W., Lundin, E.R. and Ritchie, J.D. (eds). The Nature and Origin of Compression in Passive Margins. *Geological Society of London Special Publications*, 306, 121-136.

Saunders, A.D., Fitton, J.G., Kerr, A.C., Norry, M.J. and Kent, R.W. 1997. In Mahoney, J.J. and Coffin, M.F. (eds). The North Atlantic Igneous Province. *American Geophysical Union, Geophysical Monograph*, 100, 45-93.

Scotchman, I.C. 2001. Petroleum geochemistry of the Lower and Middle Jurassic in Atlantic margin basins of Ireland and the UK. *Geological Society London Special Publications*, 188, 31-60.

Scotchman, I. C., Carr, A. D. and Parnell, J. 2006. Hydrocarbon generation modelling in a multiple rifted and volcanic basin: a case study in the Foinaven Sub-basin, Faroe-Shetland Basin, UK Atlantic margin. *Scottish Journal of Geology*, 42, 1-19.

Shannon, P.M., Jacob, A.W.B., O'Reilly, B.M., Hauser, F., Readman, P.W. and Makris, J.1999. Structural setting, geological development and basin modelling in the Rockall Trough. *In*: Fleet, A.J. and Boldy, S.A.R. (Eds.), *Petroleum Geology of Northwest Europe: Proceedings of the 5th Conference*, Geological Society, London, 42-43.

Shaw, F., Worthington, M.H., White, R.S., Andersen, M.S. and Petersen, U.K. 2008. Seismic attenuation in Faroe Islands basalts. *Geophysical Prospecting*, 56, 5-20.

Smallwood, J.R. 2009. Back-stripped 3D seismic data: a new tool applied to testing sill emplacement models. *Petroleum Geoscience*, 15, 259-268.

Spitzer, R., White, R.S. and Christie, P.A.F. 2008. Seismic characterisation of basalt flows from the Faroes margin and the Faroe-Shetland Basins. *Geophysical Prospecting*, 56, 21:31.

Tate, M. P., Dodd, C. D. and Grant, N. T. 1999. The Northeast Rockall Basin and its significance in the evolution of the Rockall-Faeroes/East Greenland rift system. Fleet, A.J. and Boldy, S.A.R. (eds.) Petroleum Geology of Northwest Europe, Proceedings of the 5*th*. Conference, Geological Society, London: 391-406.

White, R.S., Fruehn, J., Richardson, K.R., Cullen, E., Kirk, W., Smallwood, J.R. and Latkiewicz, C. 1999. Faroes Large Aperture Research Experiment (FLARE): imaging through basalt *In*: Fleet, A.J., Boldy, S.A.R. (eds) *Petroleum Geology of Northwest Europe: Proceedings of the 5th Conference*: 1243-1252.

White, R.S., Smallwood, J.R., Fliedner, M.M., Boslaugh, B., Maresh, J. and Fruehn, J. 2003. Imaging and regional distribution of basalt flows in the Faeroe-Shetland Basin. *Geophysical Prospecting*, 51: 215-231.

White, R.S., Spitzer, R., Christie, P.A.F., Roberts, A., Lunnon, Z., Maresh, J. and iSIMM Working Group. 2005. Seismic imaging through basalt flows on the Faroes Shelf. Proceedings of the 1*st* Faroe Islands Exploration Conference. Annales Societatis Scientiarum Færoensis, Supplementum 43, Tórshavn: 11-31.

Ziska, H. and Andersen, C. 2005. Exploration Opportunities in the Faroe Islands. Proceedings of the 1 Faroe Islands Exploration Conference: Proceedings of the 1*st* Conference, Annales Societatis Scientiarum Færoensis, Supplementum 43: 146-162.

The Wyville Thomson Ridge Complex located in the NE Atlantic – Aspects of the Tertiary development

INGUN ZISKA NIELSEN[1] AND LARS OLE BOLDREEL[2]

[1] Geological Survey of Denmark and Greenland, Østervoldgade 10, 1350 København K, Denmark
E-mail: izn@geus.dk; Tel: +45 38142563

[2] University of Copenhagen, Department of Geography and Geology, Østervoldgade 10, 1350 København K, Denmark.

Abstract

The Wyville Thomson Ridge Complex (WTRC) located in the NE Atlantic is a major anticline compound that has been investigated by interpreting modern commercial 2D digital reflection seismic data. The complex constitutes of Wyville Thomson Ridge (WTR) and the Ymir Ridge (YR) and is so far undrilled. It is proposed that the orientation of the apex alongside the WTR and the YR changes direction; the WTRC tilted towards the southeast; the WTRC experienced a clockwise rotation from Late Paleocene until Middle Miocene; the WTRC is segmented by two ENE/WSW trending fissures and adjacent NE/SW trending transfer faults; beneath the south eastern part of the Ymir Ridge a transcurrent fault ends as a listric fault in the Rockall Basin. Four compressional phases affected the WTRC 1) Late Paleocene - Early Eocene 2) Early Eocene 3) Early Oligocene and 4) Middle Miocene. Based on the seismic interpretations a structural model is presented.

Introduction

The objective of this paper is to present a simple structural model accounting for all the diverse stress regimes and resulting strain that have been involved in the post volcanic evolution of the Wyville Thomson Ridge Complex (WTRC) (Fig. 1). This was obtained by resolving the Tertiary movement of WTRC, by interpretation of the post basalt sediments from 2D modern reflection seismic profiles (Fig. 1). The seismic interpretation was correlated to the nearby areas. In order to construct the model the stratigraphic development of the basins next to the Wyville Thomson Ridge (WTR) and Ymir Ridge (YR) was analysed.

Geological Setting

Since the collapse of the Caledonides during the late Silurian – Early Devonian (Archer *et al.*, 2005) several episodic, non-magmatic extension phases occurred in the area with the NE Atlantic margin resulting in a wide rifted region (Lundin and Doré, 2005) bearing the NE-SW Caledonian trend (e.g. Archer *et al.*, 2005). Within the Faroe-Shetland, Rockall and Porcupine areas at least six main phases of rifting events have been described (Dean *et al.*, 1999): (1) Devonian – Carboniferous (2) Permian – Triassic (3) Middle Jurassic (4) Late Jurassic (5) Cretaceous and (6) Paleocene.

During Hauterivian (Early Cretaceous c. 135-

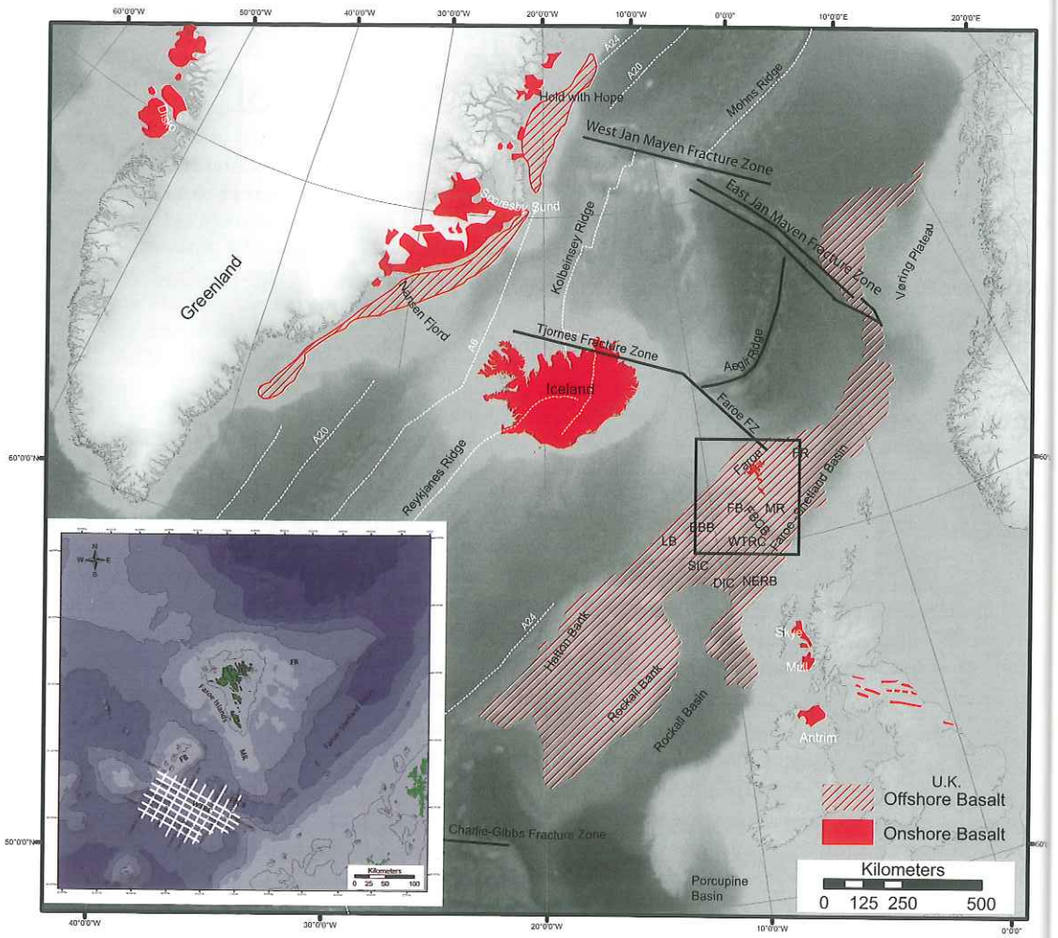

Fig. 1.
Geographical map of the North Atlantic including structural features in the region: the North Atlantic Igneous Province (NAIP) extends from Baffin Islands (not shown) and to the northern part of the British Isles (Adapted from Ritchie *et al*., 1999, Frei, 2005 and Ganerød *et al*. 2008). The bathymetry data is the ETOP01 data set (Amante and Easkins, 2008). Faroe Fracture Zone and Tjörnes Fracture Zone (redrawn from Kimbell *et al*., 2005). BBB, Bill Bailey Bank; DIC, Darwin Igneous Centre; FB, Faroe Bank; FBCB, Faroe Bank Channel Basin; FR, Faroe Ridge; LB, Lousy Bank; MR, Munkagrunnur Ridge; NERB, North East Rockall Basin; SIC, Sigmundur Igneous Centre; WTRC, Wyville Thomson Ridge Complex. The seismic survey YMR97 investigated in this study is visualized in the insert figure.

132 Ma) the extensional stress direction shifted from E-W to NW-SE (Doré *et al*., 1999) when the southerly propagating Arctic rift (consisting of the Faroe-Shetland-Møre basins) united with the northerly propagating Atlantic rift (consisting of the Rockall Basin) forming a single, linked rift system (Roberts *et al*., 1999) (Fig. 1). Oceanic spreading and voluminous and widespread volcanism accompanied the rift phases culminating with the separation of Greenland and Eurasia (e.g. Saunders *et al*., 1997). The North Atlantic seafloor spreading started in Aptian time (middle

Early Cretaceous c. 118 Ma) between Newfoundland and Bay of Biscay/Iberia representing a weak NE-SW extensional stress direction (Lundin and Doré, 2005).

Rifting between Greenland and Eurasia, including the Faroe-Rockall Plateau (Boldreel and Andersen, 1993) plus the Jan Mayen microcontinent (Hinz *et al*., 1993; Eldholm and Thiede, 1980) initiated in Paleocene (57-56 Ma Chron 24/25) (Larsen, 1988) or (c. 56-53 Ma) (Saunders *et al*., 1997). The simultaneous rifting on each side of Greenland, in the Labrador Sea/Baffin Bay and the NE Atlantic, was linked at a triple junction south of Greenland (Lundin and Doré, 2005). The ocean spreading in the Labrador Sea slowed and stopped in Middle – Late Eocene between Chrons 21 and 13 (c. 50 Ma until 36 Ma) (Saunders *et al*., 1997) but Chron 13 also marks the initiation of a continuous spreading axis between the Arctic and the NE Atlantic (Lundin and Doré, 2005). Oceanic spreading between the Faroe Fracture Zone (Bott, 1985) and the Jan Mayen Fracture Zone transferred north-westwards from the Aegir Ridge to the Kolbeinsey Ridge crossing the Jan Mayen Ridge (Fig. 1) isolating the Jan Mayen microcontinent (e.g. Nunns, 1983). Some disagreement exist on the timing of this event: from the initiation of break-up in Paleocene – Early Oligocene (Chron 24 c.54 Ma until Chron 12 c.32 Ma) when the Aegir Ridge was abandoned (Lundin and Doré, 2005), Middle Eocene – Early Miocene (Chron 22-20 until Chron 6) (Larsen, 1988), Late Eocene – Oligocene until Early Miocene (Chron 20 until Chron 7) (e.g. Nunns, 1983) or Late Oligocene (Chron 7 c.25 Ma until Chron 6) at the culmination of the Jan Mayen microcontinent separating from Greenland (Hinz *et al*., 1993; Eldholm and Thiede, 1980).

This ridge transition caused the Jan Mayen microcontinent to rotate approximately 8° anticlockwise relative to East Greenland and NW Europe (Boldreel and Andersen, 1993) and is well recorded by the difference in the orientation between the Tjörnes and Faroe Fracture Zones (Kimbell *et al*., 2005) and between the West- and East Jan Mayen Fracture Zone making up the Jan Mayen Fracture Zone (Fig. 1) (Talwani and Eldholm, 1977). This ridge transition resulted in a change in the relative motion of Greenland and Eurasia from approximately normal to the mid-ocean ridge, constituting of the Reykjanes Ridge south of Iceland and the Kolbeinsey Ridge to the north, to the spreading that persists to the present day. This spreading ridge was accomplished by utilization of the Caledonian suture zone and can be viewed as the natural consequence of the Pangaean break-up (Lundin and Doré, 2005). The rotation of the Jan Mayen microcontinent was manifested on the Faroe-Rockall Plateau (Boldreel and Andersen, 1993) where the Late Eocene unconformity developed within the Hatton Bank area (Johnson *et al*., 2005), the Rockall Basin, the north Faroe-Shetland and North Sea Fan-Vøring areas as the intra-Miocene unconformity (constituting of both Late Eocene and Base Neogene due to stratigraphic inter-correlation uncertainty over the WTRC) (Stoker *et al*., 2005).

The rifted continental margin between Greenland and Eurasia experienced the influence of the Icelandic hotspot around 64 Ma (Archer *et al*., 2005) that produced abundant igneous activity (e.g. Smith *et al*., 2005) with an overall melt estimation of 5-10 x 10^6 km^3 that was generated in only 2 Ma (White *et al*., 1987) and is referred to as the North Atlantic Igneous Province (NAIP) (e.g. Saunders *et al*., 1997; Keser Neish and Ziska, 2005). The volcanic activity on Faroe Islands lasted 4 to 7 million years mainly in the Thanetian and ceased before the opening of the NE Atlantic during Chron 24R close to the Paleocene/Eocene boundary (Waagstein, 1988). The Faroese onshore basalts are subdivided into three separate formations: The Beinisvørð Fm (Passey and Bell, 2007) (>3000 m) that extruded during Chron 26R to Chron 25N and is present over most of the Faroe-Rockall Plateau (Waagstein, 1988). The Beinisvørð Fm is overlain by the Malinstindur Fm (Passey and Bell, 2007) (~1400 m) (Waagstein, 1988) that is overlain by the Enni Fm (Passey and Bell, 2007) (~900 m) (Waagstein, 1988) and both extruded during Chron 24R and are confined to a relative narrow area along the

Stratigraphic Correlation Diagram around the WTRC						
Author/Area / Epoch	Present Article	STRATAGEM Partners, 2002	Sørensen, A. B., 2003	Andersen et al, 2000	Tate et al., 1999	Boldreel & Andersen, 1993
	WTRC	South Western Faroe-Shetland Channel	Faroese area	Eastern Faroe region	NE Rockall Basin	Faroe-Rockall area
Pleistocene	16	FSN-1	D3	FPC-D.3	9	Pliocene – Pleistocene
	12		Glacial	CN-050		
Pleistocene – Middle Pliocene	15 14 *		D2	FPC-D.2		
	11	GU/INU	Pliocene	CN-040		Late Miocene
Early Pliocene – Late Miocene	12 10 11 13	FSN-2	D1a + D1b	FPC-D.1		Late Mid Miocene
	9		Mid Miocene	CN-030		Mid Miocene
Early Miocene	10		C	FPC-C		Early Miocene
	8	TPU	Top Oligocene	CN-010	Mid Oligocene	Late Oligocene
Early Oligocene	8 7 7 9	FSP	Oligocene	FPC-B.4	8	Late Eocene – Oligocene
	6		Top Eocene	CP-100	Top Eocene	Eocene – Oligocene
Middle Eocene	6		Mid Eocene	FPC-B.3	7	Mid – Late Eocene
	5		Mid Eocene	CP-060	Mid Eocene	Intra Eocene
Early Eocene	5 4 4 3 3		Early Eocene	FPC-B.2	6	Early Eocene
	2		Top Balder Fm, T50	CP-030	Violet	
	2 1 1		Middle & Upper Basalt Series, Top Basalt, Balder Fm, Balder Tuff	FPC-B.1 tuff + Balder Fm	5 Balder Fm + tuff	
	Top Basalt			CP-010 Top Basalt	Top Basalt	
	Late Paleocene, SS, DS, FBCK and Drekaeyga Intrusion			FPC-A	4a basalt + tuff	
			Top Paleocene, T40 – T45		Brown	Paleocene – Eocene
Late Paleocene			Middle & Upper Basalt Series, T38 – T40		4b basalts	Middle & Upper Basalt Series
					Base Basalt	
					3	

Fig. 2.
A stratigraphic correlation diagram visualizing geological time versus geological locations adjacent the investigated area interpreted by different authors, showing successions (white) and their bounding unconformities or conformable reflectors/seismic key markers (pale green). T numbers are BP sequences. Numbers in the column "Present Article " refere to the interpreted seismic stratigraphic units in the present study. *Unit 14 is deposited in the AB and due to erosion the lower boundary is reflector 9. See section „Summarizing the three Sub Areas" for further details.

continental margin. The Prestfjall Fm (Passey and Bell, 2007) previously called the coal-bearing sequence (Waagstein, 1988) and the Hvannhagi Fm (Passey and Bell, 2007) also belongs to the Chron 24R and separates the Beinisvørð Fm and the Malinstindur Fm (Waagstein, 1988).

It is generally accepted that the Icelandic hotspot was the location for the break-up in the NE Atlantic, but Lundin and Doré (2005) investigated alternative origins as a consequence of plate tectonics. The NAIP was divided into two pulses (e.g. Saunders *et al.*, 1997) due to the timing and amount of the magmatic eruption, plus that the location of these magmatic areas for a specific

time interval trended almost perpendicular to one another.

The first pulse was in Middle Paleocene (c. 62-58 Ma) and mainly confined to continent-based magmatism in the form of intense dyke swarms in the British Tertiary Igneous Province (Archer *et al.*, 2005) also called the British Volcanic Province (BVP), West Greenland and eastern Baffin Bay governed by a short-lived attempt at seeking a new rift path (Fig. 1). This NW-SE belt called the Thulean Volcanic Line (Hall, 1981) indicate a NE-SW extensional stress field during part of the Paleocene (England, 1988) probably enhanced by the Pyrenean phase of the Alpine collision that was replaced as stretching and subsequent separation refocused on the NE Atlantic margin in the later Paleocene – Early Eocene (Archer *et al.*, 2005).

The second pulse was in latest Paleocene – earliest Eocene (c. 56-53 Ma) with voluminous magmatism along the NE Atlantic margins related to the final break-up of Pangaea, exploiting the collapsed Caledonian fold belt (Archer *et al.*, 2005).

Several post break-up compressional phases took place in the NE Atlantic margin and generally the Eocene – Miocene compressional phases, in form of basin inversion observed in major basins in NW Europe, are assumed to be related to the Alpine deformation (e.g. Ziegler 1987). Within the Faroe-Shetland and Hatton-Rockall areas three compressional/transpressional phases, developing major anticlinal folds, are identified: (1) Late Paleocene (Thanetian) – Early Eocene, gravitational ridge push from the N (Boldreel and Andersen, 1993) forming the WNW-trending WTRC and the NNW-trending Munkagrunnur Ridge, and the ENE-trending Fugloy Ridge might also have been active (Boldreel and Andersen, 1994) (2) Oligocene, gravitational ridge push from the NNW (Boldreel and Andersen, 1993) developing NE- to ENE-trending fold axis to the east of the Faroe Islands and in the area between Faroe Islands and Hatton Bank (Boldreel and Andersen, 1994), and at the WTRC erosional truncations are seen on the Late Oligocene unconformity (Boldreel and Andersen, 1993) and (3) Middle – Late Miocene, gravitational ridge push from the NW developing WSW-ENE to SW-NE-trending anticlines in the FSB plus almost E-W-trending structures in the Faroe Rockall Plateau (Boldreel and Andersen, 1993). However, Andersen *et al.* (2002) only recognised two major compressional phases in the Faroe Platform area (1) Middle Eocene and (2) Middle – Late Miocene times. Many scenarios have been described in the attempt to explain the genesis of the WTR and the YR and therefore also of the WTRC e.g. Boldreel and Andersen (1993), Johnson *et al.* (2005), Keser Neish and Ziska (2005), Kimbell *et al.* (2005), Smith *et al.*, (2009), Stoker *et al.* (1993) and Tate *et al.* (1999).

Materials and Methods

In 1997 Fugro-Geoteam AS recorded a 2D seismic survey YMR97 (1782 line km) SW of the Faroe Islands. The source type was a G-Gun 3040 Cu. inch array fired at a depth of 8 m below the sea surface and at an interval of 25 m. The 6 km long cable, placed in 10 m depth in the water with an offset of 140 m, contained 480 channel groups with a group length of 12.5 m and the CDP interval was 6.25 m. The recorded length was 8 sec. with a 2 msec. sample rate, filters of a Low-cut 4 Hz and a High-cut 204 Hz, and the data were stored as normal polarity in a SEG-D 8015 format. Afterwards Robertson Research International LTD. processed the data to zero phase signal with a CDP gather of 120 fold and used the Kirchhoff summation migration method.

The criteria applied for reflector interpretation has been to define the base of each seismic unit on the 16 profiles used. The seismic profiles were thus thoroughly interpreted as a large numbers of reflectors and units have been analysed.

The investigated area was divided into three sub areas named the Rockall Basin (RB), Auðhumla Basin (AB) and Faroe Bank Channel Basin (FBCB) located from the south towards the north (Fig. 1). The three sub areas were interpreted independently and afterwards the

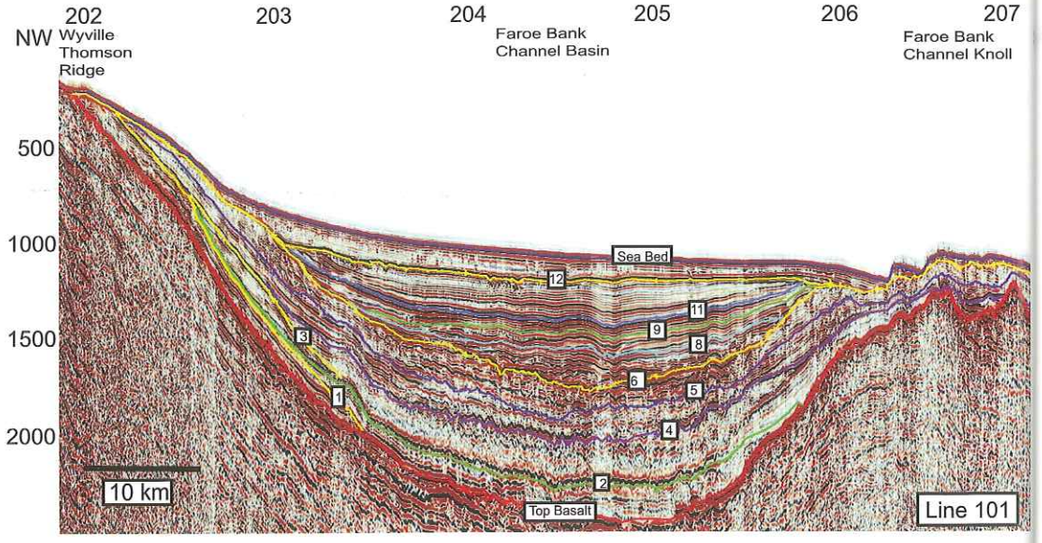

Fig. 3.
The key profile chosen in the FBCB is the WNW-ESE seismic line 101 approximately 161 km long. 11 reflectors were interpreted and 11 units analysed and are referred to in the text. The depth in ms TWT and the crossing seismic lines are shown. To the NW the upper part of the WTR is eroded. On the WTR north western flank adjacent to line 203 two small bulges are expressed at the Top Basalt that continues until the reflector 6. The sedimentary units below reflector 6 display a chaotic seismic pattern whereas the younger units show a non chaotic seismic character with a similar geographical extent of the depositional area.

interpretation was merged from south to north. A direct correlation can be established between the interpreted reflectors in the RB and the AB, but a similar connection is not possible between the AB and the FBCB. To assign age relation to the interpreted reflectors STRATAGEM Partners (2002), Sørensen (2003), Andersen *et al.* (2000), Tate *et al.* (1999) and Boldreel and Andersen (1993) were used for correlation (Fig. 2).

Three interpreted key seismic profiles (Figures 3, 4 and 5) representing each sub area and one profile (Fig. 6) that intersects the sub areas are shown in order to illustrate the connection and correlation of the development in the sub areas. The profiles that represent the RB and the FBCB are located high on the flanks of the ridges, and therefore reflect the deposition of the sediment packages located on the flanks rather than in the basins. The profile in the AB is located in the centre of the basin. The seismic units are named after the upper reflector demarcating the units.

Results

Top Basalt

The top of the basalt is a high amplitude peak reflector in the entire survey and a depth map to the surface of the basalt is produced (Fig. 7). The interpretation shows that the basalt in places is eroded at the apex of the WTR and the YR, and that the orientation of the apex alongside both ridges changes.

Faroe Bank Channel Basin - Observations of the Seismic Units

In the Faroe Bank Channel Basin the seismic line 101 (Fig. 3) was chosen as the key profile.

FBCB Unit 1– FBCB Unit 5

FBCB Unit 1 is at the lower boundary limited by reflector Top Basalt and at the upper boundary by reflector 1. Reflector 1 is characterized as a high amplitude peak that downlaps the Top Basalt reflector in the basinwards direction. The external form of FBCB Unit 1 is a prograding wedge. The internal reflection pattern consists of subparallel downlapping reflectors of high amplitude and frequency and truncations occur at the top of FBCB Unit 1 towards the WTR. The unit has a limited extent as it is present only at the intersecting of line 202, 203 and 101.

FBCB Unit 2 is at the lower boundary limited by reflector Top Basalt and at the upper boundary by reflector 2. Reflector 2 is a high amplitude trough that onlaps the Top Basalt reflector and downlaps the Top Basalt reflector basinwards. The external form of FBCB Unit 2 is a basin fill. In the NW the internal pattern is at the lower part represented by onlapping high amplitude and frequency subparallel continuous reflectors and truncation occurs in the upper part. Basinwards the pattern becomes chaotic to contorted and lower amplitude and frequency is observed as compared to the NW. The unit is found in most of the FBCB.

FBCB Unit 3 is at the lower boundary limited by reflector 2 and at the upper boundary by reflector 3. Reflector 3 is a high amplitude trough and onlaps reflector 1 towards the WTR and downlaps reflector 2. The external form of FBCB Unit 3 is a prograding wedge. The internal pattern is continuous subparallel reflectors of medium to high amplitude and low to high frequency. The unit is limited to the intersection of line 203 and 101.

FBCB Unit 4 is at the lower boundary limited by reflector 2 and at the upper boundary by reflector 4. Reflector 4 is a high amplitude undulating trough that onlaps the older boundaries. The external form of FBCB Unit 4 is a basin fill. The internal pattern is onlapping subparallel continuous reflectors of medium to high amplitude and low to medium frequency that become disrupted in the central part of the FBCB. The unit is found in FBCB apart from FBCK.

FBCB Unit 5 is at the lower boundary limited by reflector 4 and at the upper boundary by reflector 5. Reflector 5 is a low amplitude peak that onlaps reflector 4 and in the north western area reflector 3. The external form of FBCB Unit 5 is a basin fill. The internal pattern consists of onlapping subparallel continuous reflectors of medium to high amplitude and low to medium frequency. The unit is found in FBCB apart from the FBCK.

FBCB Unit 6

FBCB Unit 6 is at the lower boundary limited by reflector 5 and at the upper boundary by reflector 6. Reflector 6 is a high amplitude peak that is truncated at the top of FBCB Unit 6 in the NW. The external form of FBCB Unit 6 is a basin fill. The internal pattern is onlapping subparallel continuous reflectors of medium to high amplitude and low to medium frequency. The unit is found in FBCB apart from the FBCK.

FBCB Unit 7

FBCB Unit 7 is at the lower boundary limited by reflector 6 and at the upper boundary by reflector 8. Reflector 8 is a high amplitude peak that onlaps reflector 6. The external form of FBCB Unit 7 is a basin fill changing into a prograding wedge on line 206. The internal pattern shows high amplitude and medium to high frequency continuous subparallel reflectors. The unit is present in the area where lines 202-206 intersect 101.

FBCB Unit 8

FBCB Unit 8 is at the lower boundary limited by reflector 8 and at the upper boundary by reflector 9. Reflector 9 is a high amplitude peak that onlaps reflector 8 towards the NW and seems to onlap reflector 6 close to the FBCK. The external form of FBCB Unit 8 is a prograding basin fill changing into a prograding wedge close to the FBCK. The internal pattern is characterized of high amplitude and medium to high frequency by onlapping continuous subparallel reflectors, although downlap is observed adjacent the FBCK. The unit is found in the area where lines 203-206 intersect 101.

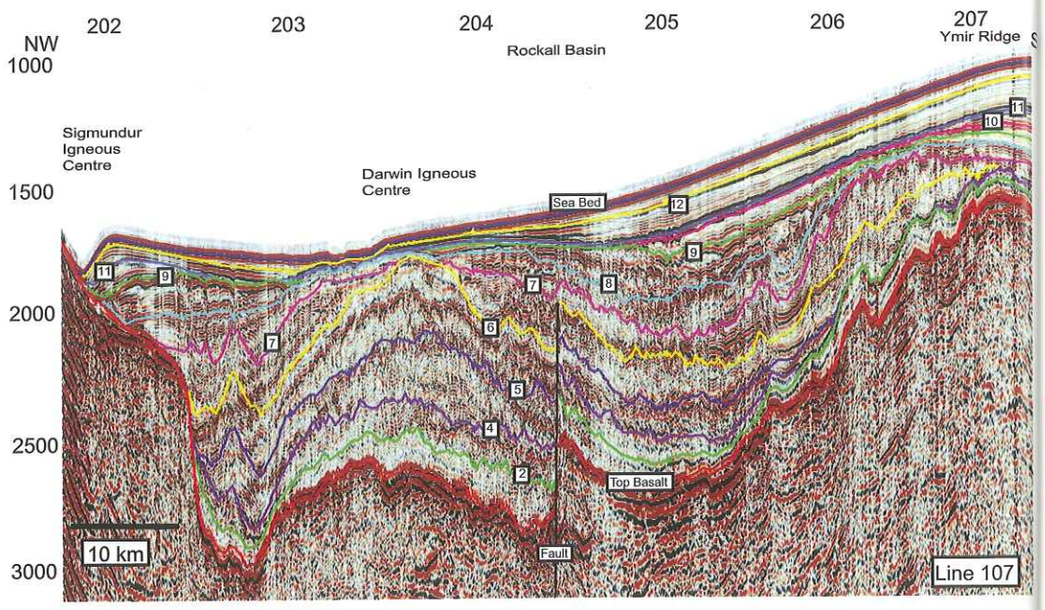

Fig.4.
The key profile chosen in the RB is the approximately 120 km long WNW-ESE seismic line 107 along with 11 reflectors interpreted and 11 units analysed. The depth in ms TWT and the crossing seismic lines are shown. The Sigmundur Igneous Centre (SIC) is located in the NW with the adjacent Darwin Igneous Centre (DIC) and ending with the YR in the SE. The SIC is demarcated by an escarpment and the flank of DIC towards the north is demarcated by a fault being active until Early Oligocene. The lava flows that originate from the SIC show onlap to the lava flows from the DIC in a SE direction. Above the DIC, between the SIC and the fault, the sediments up to Top Oligocene are squeezed and bulging upwards as a dome indicating compression. SE of the fault the only indication of compression is a few bulges adjacent to line 206 at the Top Basalt that continues in the sedimentary units until the Top Oligocene.

FBCB Unit 9

FBCB Unit 9 is at the lower boundary limited by reflector 9 apart from the NW where the lower boundary is reflector 6, and is at the upper boundary limited by the reflector 11. Reflector 11 is a high amplitude trough that onlaps the lower boundary. The external form of FBCB Unit 9 is an onlapping basin fill changing into a prograding wedge close to the FBCK. The internal pattern constitutes of onlapping continuous subparallel reflectors of high amplitude and medium to high frequency, however downlap is observed adjacent the FBCK. The unit is found in the area where the lines 203-206 intersect 101.

FBCB Unit 10

FBCB Unit 10 is at the lower boundary limited by reflector 11 and at the upper boundary by reflector 12. Reflector 12 is a high amplitude trough that onlaps the lower boundary. The external form of FBCB Unit 10 is a prograding basin fill changing into a prograding wedge close to the FBCK. In the NW the internal pattern is represented by onlapping continuous subparallel reflectors of medium to high amplitude and low to high frequency and truncations are found at the top of FBCB Unit 10 in the NW. Adjacent the FBCK the internal pattern shows onlapping reflectors that basinwards downlap the lower boundary of medium amplitude and low to medium frequency. The unit is present in the area of intersecting lines 203-209 with the 101 apart from the FBCK.

FBCB Unit 11

FBCB Unit 11 is at the lower boundary limited by reflector 12 and at the upper boundary by reflector Sea Bed. Reflector Sea Bed is a high amplitude peak in the entire survey. The external form of FBCB Unit 11 is a basin fill. The internal pattern consists of onlapping continuous subparallel reflectors of medium to high amplitude and low to high frequency. The unit is present in the whole FBCB.

Interpretations of the Seismic Units

Early Eocene

FBCB Unit 1 has a limited areal distribution and is reasonable thin (Fig. 3). This indicates that a small amount of clastic material, as judged from the internal reflector pattern, may originate from the north western part of the WTR. It is interpreted that the relative sea level fell to allow for erosion of the flood basalt in the NW of the WTR. This relative sea level fall indicates the first uplift of the WTR as the unit is found only in the NW. This shows that the WTR did not act as one continuous ridge and thus it seems to be segmented.

FBCB Unit 2 consists of material that seems to originate from the WTR. The unit is extensive distributed in the basin and indicates that abundant depositional material was available (Fig. 3). To the NW the unit is deposited higher up the flank of the WTR than in the SE indicating that the WTR is segmented. The distribution of the unit indicates a relative sea level rise due to basin subsidence before and during the deposition.

FBCB Unit 3 has a limited areal distribution (Fig. 3) and indicates that a small amount of material which may well originate from the NW of the WTR. Before and during deposition of the unit the relative sea level fell to allow for erosion of the flood basalt in the NW of the WTR. The relative sea level fall indicates the second uplift of the WTR. The extent of the unit shows that the WTR is segmented, and that the basin subsided towards the SE.

FBCB Unit 4 is found in the whole FBCB apart from the FBCK and indicates that abundant material, as indicated by the internal reflector pattern, may originate from the WTR (Fig. 3). To the SE the unit is deposited higher up the flank of the WTR than to the NW indicating that the WTR is segmented. The distribution of the unit indicates a relative sea level rise caused by basin subsidence before and during the deposition.

FBCB Unit 5 consists of material that seems to originate from the WTR and onlaps reflector 1 near the sea bed to the NW as judged from the internal reflector pattern (Fig. 3). The Early Eocene reflector represent the first compressional phase, as all the previous units can be seen as an continuation of the same development resulting in a compressional phase.

Middle Eocene

FBCB Unit 6 has the widest distribution among all the units. Approximately midway on the inclination of the WTR the reflectors show progradation and aggradation from the WTR (Fig. 3) signifying a fast depositional rate. Before and during the deposition of the unit the relative sea level rose due to basin subsidence.

After deposition of the reflector 6 the relative sea level fell and caused a break in sedimentation indicated by the erosion of the entire upper boundary of FBCB Unit 6. This relative sea level fall marks the Top Eocene unconformity and indicates the third uplift of the WTR.

Early Oligocene

FBCB Unit 7 is recognized in the deepest part of the basin (Fig. 3) and may originate from the WTR. The internal reflectors onlap reflector 6 and indicate an enhanced accommodation space during deposition of the unit caused by basin subsidence and a relative sea level rise.

Early Miocene

FBCB Unit 8 is found in the deepest part of the

basin and may originate from the WTR as judged from the internal reflector pattern (Fig. 3). The unit thickens basinwards and indicates that the accommodation space and the relative sea level were about the same or slightly enlarged as in the deposition of FBCB Unit 7.

Late Miocene – Early Pliocene

FBCB Unit 9 appears in the deepest part of the basin adjacent the FBCK and the internal reflector configuration is downlap (Fig. 6). The relative sea level was about the same or slightly rising as the basin continued subsiding leading to a slightly enhanced accommodation space.

Middle Pliocene – Pleistocene

FBCB Unit 10 is recognized in the deepest part of the basin and as based on the seismic interpretations originated from the WTR. The internal reflectors onlap reflector 11 in the NW (Fig. 3) but downlap on reflector 11 in the SE (Fig. 6). The accommodation space was slightly enhanced as the unit reaches further op the WTR than the previous unit and indicates a relative sea level rise caused by basin subsidence.

After deposition of FBCB Unit 10 a relative sea level fall occurred causing a break in sedimentation indicated by the erosion of the entire upper boundary of the unit (Fig. 3). The erosion was more severe in the NW where all reflectors show truncation and may be caused by one or more of the following 1) the accommodation space was filled up 2) strong sea currents initiated 3) glaciation began 4) only the NW of the WTR was uplifted indicating that the WTR is separated by faults or transfer zones. The relative sea level fall marks the Glacial Unconformity and indicates the fourth uplift of the WTR.

Pleistocene

During deposition of FBCB Unit 11 the basin subsided and this indicates a relative sea level rise.

Rockall Basin - Observations of the Seismic Units

In the Rockall Basin the seismic line 107 (Fig. 4) was chosen as the key profile.

RB Unit 1 – RB Unit 3

RB Unit 1 is at the lower boundary limited by reflector Top Basalt and at the upper boundary by reflector 2. Reflector 2 is an onlapping undulating trough. The external form of RB Unit 1 is a basin fill. The internal pattern is chaotic to contorted onlapping reflectors of medium amplitude and low to medium frequency. The unit is present in the RB apart from a fault in an area where the line 106 intersects line 204.

RB Unit 2 is at the lower boundary limited by reflector 2 and at the upper boundary by reflector 4. Reflector 4 is a high amplitude undulating trough that onlaps the top basalt. The external form of RB Unit 2 is a basin fill. The internal pattern is represented by onlapping chaotic to contorted reflectors of medium amplitude and low to medium frequency. The unit is present in the RB apart from the area where the lines 204 and 106 intersect due to a fault and in the area with intersecting lines 206-207 with 106-107 as a compression bulge is found here (See Fig.1 for seismic line location).

RB Unit 3 is at the lower boundary limited by reflector 4 and at the upper boundary by reflector 5 (Fig. 4). Reflector 5 is a low to medium amplitude undulating peak onlapping the lower boundary. The external form of RB Unit 3 is a basin fill. The internal pattern is chaotic to contorted onlapping reflectors of low to high amplitude and frequency. The unit is found in the whole RB apart from the SE where line 207 intersects line 107.

RB Unit 4

RB Unit 4 is at the lower boundary limited by reflector 5 and at the upper boundary by reflector 6. Reflector 6 is a low to high amplitude undulating peak that onlaps the top basalt at the YR and reflector 5 in the SE. The external form of RB Unit 4 is a basin fill. The internal pattern is chaotic to contorted onlapping reflectors of low to high amplitude and frequency. The unit is present in the whole RB.

RB Unit 5 – RB Unit 6

RB Unit 5 is at the lower boundary limited by reflector 6 and at the upper boundary by reflector 7. Reflector 7 is a low to medium amplitude undulating peak that onlaps the top basalt towards the YR and reflector 6 to the SE. The external form of RB Unit 5 is a basin fill. The internal pattern shows onlapping chaotic to contorted reflectors of low to high amplitude and frequency. The unit is present in the RB apart from minor patches.

RB Unit 6 is at the lower boundary limited by reflector 7 and at the upper boundary by reflector 8. Reflector 8 is a low to medium amplitude undulating peak that onlaps the top basalt towards the YR and reflector 7 to the SE (Fig. 4). The external form of RB Unit 6 is a basin fill. The internal pattern shows onlapping reflectors that vary from subparallel and chaotic to contorted, all of low to high amplitude and frequency. The unit is present in the RB apart from an area where lines 205-207 intersect line 106 (Fig. 1).

RB Unit 7

RB Unit 7 is at the lower boundary limited by reflector 8 and at the upper boundary by reflector 9. Reflector 9 is a high amplitude peak (low to high in the NW) that onlaps the top basalt towards the YR (Fig. 4), and reflector 8 in the central and SE part of the RB. The external form of RB Unit 7 is a basin fill. The internal pattern shows onlapping subparallel reflectors that are chaotic to contorted in the NW all of medium to high amplitude and low to high frequency. Truncations are found in the central and north western part except adjacent the Sigmundur Igneous Centre (SIC) and the YR. The unit is present in the RB apart from small patches.

RB Unit 8 – RB Unit 9

RB Unit 8 is at the lower boundary limited by reflector 9 and at the upper boundary by reflector 10. Reflector 10 is a medium to strong amplitude peak. The external form of RB Unit 8 is an onlapping and migrating wave basin fill. The internal pattern shows one reflector changing to three subparallel reflectors in the SE but changes to continuous subparallel reflectors in the NW all with low to medium amplitude and frequency. The unit is only found to the SE where lines 205-207 intersect line 107 (Fig. 4).

RB Unit 9 is at the lower boundary limited by reflector 10 and at the upper boundary by reflector 11. Reflector 11 is a high amplitude trough that in the NW on line 107 (Fig. 4) onlaps reflector 9. The external form of RB Unit 9 is an onlapping and migrating wave basin fill. The internal pattern shows one to two continuous subparallel reflectors in the SE changing to abundant reflectors in the NW of medium to high amplitude and low to high frequency. The unit is present in the RB apart from some minor areas.

RB Unit 10

RB Unit 10 is at the lower boundary limited by reflector 11 and at the upper boundary by reflector 12. Reflector 12 is a high amplitude trough. The external form of RB Unit 10 is a downlapping and migrating wave basin fill. The internal pattern shows continuing subparallel downlapping reflectors of medium to high amplitude and low to high frequency. The unit is present in the RB apart from an area with intersecting lines 205-207 with line 106 (Fig. 1).

RB Unit 11

RB Unit 11 is at the lower boundary limited by reflector 12 and at the upper boundary by reflector Sea Bed (Fig. 4). The Sea Bed reflector is a high amplitude peak. The external form of RB Unit 11 is a basin fill. The internal pattern shows one or two continuous subparallel downlapping reflectors of medium to high amplitude and low to high frequency. The unit is present all over the RB.

Interpretations of the Seismic Units

Early Eocene

RB Unit 1 may originate from the WTR and other surrounded elevated basaltic areas and has been exposed to compression (Fig. 4). The relative sea level fell after the volcanic activity ceased to allow for erosion of the flood basalt of the WTR and other surrounded elevated areas indicating the first uplift of the YR.

A NW/SE trending normal fault is located along the northern flank of the Darwin Igneous Centre (DIC) (Fig. 8) and RB Unit 1 is thicker to the SW than to the NE of the fault. The unit is missing in the area between the fault and YR on line 204 and on line 106 in the area from the fault to midway between lines 204 and 205. SE of line 204 the normal fault is outside the seismic survey. Located between the normal fault and the YR, a small scale foreland compressional belt is present (Fig. 8). The belt dies out or is located outside the survey on line 207 where the YR is widest. This compressional foreland belt is much smaller in size to the NW than to the SE and indicates that the two volcanic centres may have absorbed much of the compression.

RB Unit 2 may originate from the WTR and other surrounded elevated basaltic areas (Fig. 4). The unit has been subjected to compression. The relative sea level rose, but in the SE the relative sea level fell likely due to the compression that elevated the southern part of the YR thus indicating that the YR is a segmented ridge.

During deposition of RB Unit 2, deposition did not occur in two areas. The first area is described above in RB Unit 1. The second area is to the SE and is located on line 106 and 107 at the apex of YR approximately between line 206 and 207 (Fig. 8). On line 107 (Fig. 4) the unit is missing just NW of the apex indicating that the YR was exposed to a compression from the north, northeast, east or southeast resulting in a rotation of the apex towards the south, southwest, west or northwest. On line 106 the unit is missing on top of the YR and on top of the compressional foreland belt located alongside the YR further to the NW. On the intersecting line 207 the compressional foreland belt is located outside the survey but the RB Unit 2 is missing at the apex of the YR. Rotation seems not to have taken place at the location of line 207 (Fig. 4) as reflector 4 is onlapping the reflector 2 approaching the area from the RB in the SW but downlapping the reflector 2 coming from the AB in the NE. However, this area without deposition, was the apex of the YR during deposition of the RB Unit 2 and therefore, the reflector had to be deposited as an onlapping reflector. By a rotation an onlapping reflector changes into a downlapping reflector in the direction of the compression being the north, northeast or east. Where line 206 (Fig. 6) intersects the YR perpendicularly, the apex has turned towards the SW (Fig. 7) indicating that the compression originated from the NE. This NE compression is also confirmed by the flanks of the compressional belt indicating that the NE-SW direction is parallel to the compression direction. Therefore, this could correspond to the first compressional phase described as a ridge push from the north in Late Paleocene – Early Eocene (Boldreel and Andersen, 1994) although the compression direction differs slightly.

It is suggested that a transcurrent fault being an extension of the Ymir/Ness Lineament is located underneath and alongside the YR (Fig. 8) causing the ridge to wiggle about the transcurrent fault as if it was a hinge. Therefore, the upper boundary of RB Unit 1 downlaps the Top Basalt reflector coming from the RB in the SW, and reflector 4 downlaps reflector 2 coming from the AB in the NE. This indicates that after deposition of RB Unit 1 the apex of the YR was pushed towards the NE and after deposition of RB Unit 2 the apex of the YR was pushed towards the SW. Also the compression that originated from the SW had to be stronger than the compression originated from the NE as reflector 2 retained being a downlapping reflector.

The area SW of the normal fault and between the two volcanic centres (Fig. 8) subsided more than the area to the NW of the normal fault. This might be due to the location of one or several fissures as well as lava flows originating from the DIC spreading out and reaching the YR. Indications that the normal fault released much of the compressional tensions are seen.

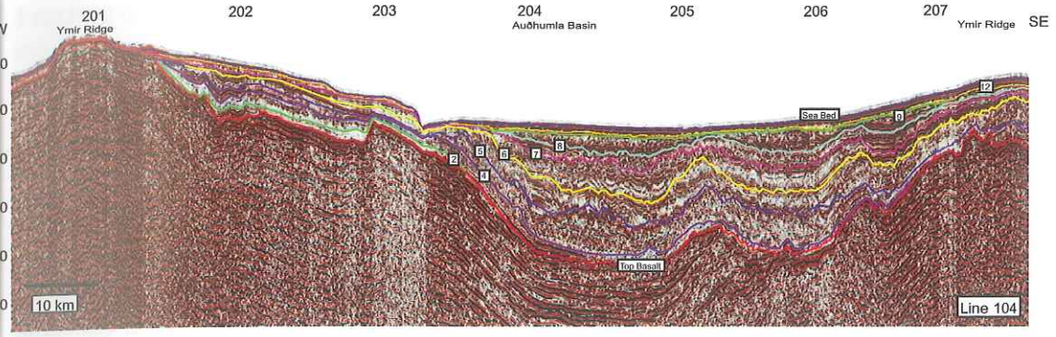

Fig.5.
The key profile chosen in the AB is the WNW-ESE seismic line 104 approximately 152 km long with 9 reflectors interpreted and 9 units analysed. The depth is ms TWT and the crossing seismic lines are shown. The bending YR is situated to the NW and the SE with the AB placed in between. In the NW an escarpment is located at the Top Basalt and between lines 205-207 two larger bulges are seen interpreted as the Drekaeyga Intrusion (DI). The sedimentary units up until reflector 9 follow the contours of the Top Basalt, and overall the sedimentary units onlap in the NW but overstep the YR in the SE. Units deposited after reflector 9 comprises sinusoidal sediment waves and contourite deposits. To the NW an erosional channel is present where sediments were eroded down into the Top Eocene unit by the Glacial Unconformity.

RB Unit 3 may originate from the WTR and surrounded elevated areas. The normal fault mentioned previously in RB Unit 2 was active during the deposition, as RB Unit 3 is slightly thicker SW of the normal fault than to the NE (Fig. 4). From line 205 towards the NW the RB Unit 3 is thicker and reaches slightly further up the YR than in the RB Unit 1 and RB Unit 2 (Fig. 4), indicating an area of subsidence that caused a relative sea level rise.

Middle Eocene

RB Unit 4 has the widest distribution among the units interpreted. The depositional material may originate from the WTR and surrounded elevated areas. The normal fault described in RB Unit 2 seems to be a strike-slip fault that ends as a listric fault in the NW (Fig. 8). During deposition of RB Unit 4 the strike-slip fault was active and the area was subjected to subsidence but not compression that caused a relative sea level rise.

After deposition of RB Unit 4 the Top Eocene unconformity occurred and eroded the entire apex of the YR due to a pronounced fall in the relative sea level and indicates the second uplift of the YR. A moat present alongside the YR is caused by erosive sea currents which may have been active at a later stage.

Early Oligocene

RB Unit 5 may originate from the WTR and surrounded elevated areas. During deposition of RB Unit 5, lack of deposition occur in the same area as described in RB Unit 1 and at the top of the dome on line 107 (Fig. 4) where the RB Unit 5 onlaps reflector 6. Thickness analyses show that the strike-slip fault was active at a time period that corresponds to about three quarters of the thickness of RB Unit 5. The lows created by the compression and erosion at the Top Eocene unconformity were infilled as the accommodation space was enhanced compared to RB Unit 4 indicating a relative sea level rise due to basin subsidence.

RB Unit 6 seems to originate from the WTR and surrounded elevated areas. Only at the top of

the YR in the SE deposits lack (Fig. 4). The RB Unit 6 oversteps the previously mentioned dome and reaches higher up the SIC and YR indicating a relative sea level rise due to basin subsidence during the deposition.

After deposition of RB Unit 6 the upper boundary was eroded due to compression, indicated by the Top Oligocene unconformity and the third uplift of the YR. In the SE part of line 107 (Fig. 4) between line 206 and 207 the apex of the YR rotated once again towards the SW and the same processes may be active as described previously in RB Unit 2. This may correspond to the second compressional phase described as a ridge push from the north-north-west in Oligocene (Boldreel and Andersen, 1994) although the compressional direction is not the same.

Early Miocene

RB Unit 7 may originate from the WTR and surrounded elevated areas. The RB Unit 7 onlaps the dome previously mentioned and the SIC western flank higher up than in RB Unit 6 (Fig. 4) and thus indicate a relative sea level rise due to basin subsidence during the deposition.

After deposition of RB Unit 7 erosion occurred and truncated the upper boundary NW of the dome due to compression and indicates the fourth uplift of the YR and a relative sea level fall. The sediments are eroded by sea bottom currents that transported and deposited the sediments as contourites and sediment waves towards the YR and the moat mentioned previously in RB Unit 4. This is the Middle Miocene unconformity and could correspond to the third compressional phase described as a ridge push from the NW in Middle – Late Miocene (Boldreel and Andersen, 1994 and Andersen *et al*, 2002).

Late Miocene – Early Pliocene

RB Unit 8 is deposited by sea bottom currents that eroded the RB Unit 7 and transported the sediments adjacent the SIC and the YR (Fig. 4) as sinusoidal sediment waves or contourite deposits filling up the moat. During deposition of RB Unit 8 the relative sea level rose due to basin subsidence but the same area as described in RB Unit 1 is left without deposition.

RB Unit 9 is deposited by sea bottom currents and transported the sediments adjacent the SIC and the YR as sinusoidal sediment waves or contourite deposits filling up the moat (Fig. 4). During deposition of the RB Unit 9 the relative sea level rose due to basin subsidence.

After the contourite deposition the sea bottom currents changed their direction or strength and a new moat developed at the flank of the YR in the NW on line 201 and 202.

Middle Pliocene – Pleistocene

RB Unit 10 seems to originate from the previously deposited units, YR, WTR and other surrounded elevated areas. The RB Unit 10 is deposited by sea bottom currents that transported the sediments adjacent the SIC and the moat at the flank of the YR as sinusoidal sediment waves or contourite deposits filling up the moats (Fig. 4). During deposition of RB Unit 10 the relative sea level rose due to basin subsidence.

Pleistocene

RB Unit 11 may originate from the WTR and other surrounded elevated areas. During deposition of RB Unit 11 the relative sea level rose due to basin subsidence.

Auðhumla Basin - Observations of the Seismic Units

In the Auðhumla Basin the seismic line 104 (Fig. 5) was chosen as the key profile.

AB Unit 1 – AB Unit 3

AB Unit 1 is at the lower boundary limited by reflector Top Basalt and at the upper boundary by reflector 2. Reflector 2 is a low to high amplitude trough and oversteps the YR in the NW on line 202 and on line 206 (Fig. 6) and line 207 into the RB. Reflector 2 onlaps reflector Top Basalt at the YR in the NW, but downlaps reflector Top Basalt between line 203 and 204 (Fig. 5). The external form of AB Unit 1 is a basin fill. The internal pattern shows onlapping subparallel continuous reflectors in the NW with high amplitude and frequency that changes into chaotic to contorted reflectors with lower amplitude and frequency towards the SE. The unit is present in the entire AB.

AB Unit 2 is at the lower boundary limited by reflector 2 and at the upper boundary by reflector 4. Reflector 4 is a high amplitude trough, that onlaps reflector 2 in the NW and reflector Top Basalt in the SE. The external form of AB Unit 2 is a basin fill. The internal pattern shows onlapping subparallel continuous reflectors that changes into chaotic to contorted reflectors towards the SE of low to high amplitude and frequency. The unit is present in the entire AB.

AB Unit 3 is at the lower boundary limited by reflector 4 and at the upper boundary by reflector 5. Reflector 5 is a low to medium amplitude undulating peak. The external form of AB Unit 3 is a basin fill. The internal pattern consists of onlapping subparallel reflectors that changes into chaotic to contorted reflectors towards the SE of low to high amplitude and frequency. In the NW on line 203 a moat is present. The unit is present all over the AB.

AB Unit 4

AB Unit 4 is at the lower boundary bounded by reflector 5 and at the upper boundary by reflector 6. Reflector 6 is a low to medium amplitude undulating peak. The external form of AB Unit 4 is a basin fill. The internal pattern shows onlapping subparallel reflectors of low to high amplitude and frequency that changes into chaotic to contorted reflectors towards the SE. Truncations are found at the upper boundary and an erosional channel is observed on line 104 (Fig. 5) between line 203 and 204. The unit is present in the AB except in one minor area.

AB Unit 5 – AB Unit 6

AB Unit 5 is at the lower boundary limited by reflector 6 and at the upper boundary by reflector 7. Reflector 7 is a low to medium amplitude undulating peak. The external form of AB Unit 5 is a basin fill. The internal pattern shows onlapping subparallel and chaotic to contorted reflectors of medium to high amplitude and frequency. Truncations are found and the erosional channel is observed on line 104 (Fig. 5). The unit is present in the AB apart from two minor patches.

AB Unit 6 is at the lower boundary limited by reflector 7 and at the upper boundary by reflector 8. Reflector 8 is a medium amplitude undulating peak. The external form of AB Unit 6 is a basin fill. The internal pattern shows onlapping subparallel and chaotic to contorted reflectors of medium to high amplitude and frequency. Truncations are found. The unit is found in the central and SE part of the AB.

AB Unit 7

AB Unit 7 is at the lower boundary limited by reflector 8 and at the upper boundary by reflector 9. Reflector 9 is a medium to high amplitude peak. The external form of AB Unit 7 is a basin fill. The internal onlapping subparallel and chaotic to contorted reflectors of pattern shows medium to high amplitude and frequency. Truncations are found. The unit is found in the central and SE part of the AB.

AB Unit 8

AB Unit 8 is at the lower boundary limited by reflector 9 and at the upper boundary by reflector 12. Reflector 12 is a high amplitude trough that downlaps the erosional channel and the moat in the NW (Fig. 4). The external form of AB Unit 8 is a basin fill. The internal pattern shows one to three reflectors of high amplitude and frequency. Truncations are found. The unit is found in the entire AB.

AB Unit 9

AB Unit 9 is at the lower boundary limited by reflector 12 and at the upper boundary by reflector Sea Bed. Reflector Sea Bed is a high amplitude peak. The external form of AB Unit 9 is a basin fill. The internal pattern shows infilling and onlapping subparallel reflectors of high

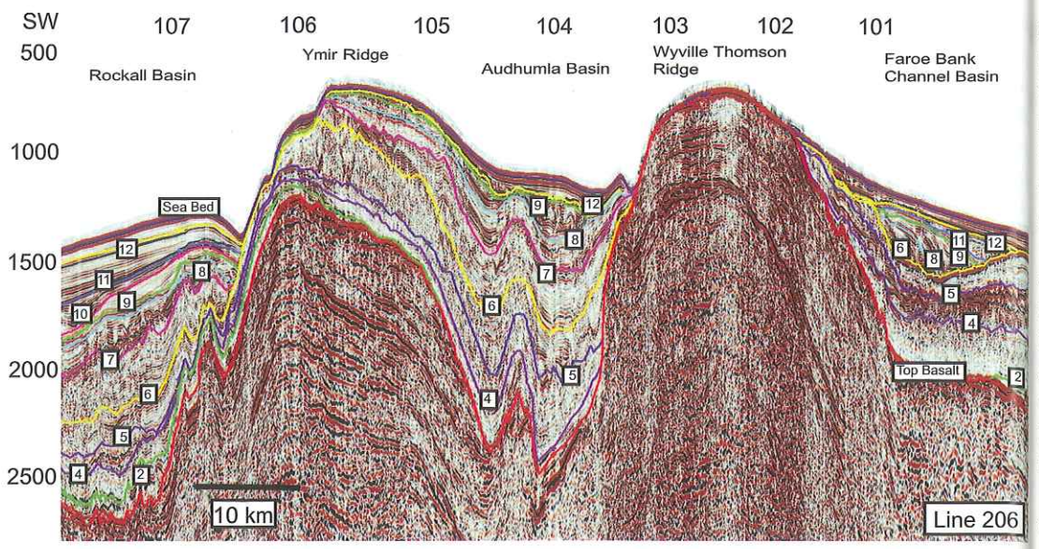

Fig. 6.
The key profile chosen for connecting the three sub areas is the NNE-SSW seismic line 206 that is approximately 103 km long where 14 reflectors were interpreted and 16 units analysed. The Depth in ms TWT and the crossing seismic lines are shown. The FBCB is different from the RB and AB and characterized by rather calm depositional conditions and was hardly affected by compressional forces. Approaching the study area from the south (RB) the four lower most units overstep the YR and continues into the AB whereas the WTR acts as a barrier and no units are directly connected to the FBCB. In the FBCB the seismic picture of the four lower most and four upper most units look similar to the four lowermost and four uppermost units in the RB. The top of the WTR show truncations and compressional structures are found in the RB and AB being active until Middle Miocene. The following pelagic units were deposited by sea bottom currents that show onlapping and migrating or sinusoidal sediment waves and contourite deposits.

amplitude and frequency. The unit is found in the entire AB.

Interpretations of the Seismic Units

Early Eocene

AB Unit 1 onlaps the Top Basalt reflector and has a limited extension in the NW and continues like a tongue along the south western side of the basin. This indicates that a small amount of likely clastic depositional material that may originate from the WTR and surrounded elevated areas was available. The relative sea level fell to allow for erosion of the flood basalt and indicates the first ridge uplift.

The deposition of AB Unit 1 indicates that the compression came from the NE, the basin was at a higher level in the NE and the compressional belt began to develop before or during the deposition of AB Unit 1. The area to the NW of the Drekaeyga Intrusion (DI) was more exposed and responsive to compression than the area SE of the DI. The deposition area of AB Unit 1 included the YR and continued into the RB. However the unit was removed by later erosion exposing the Top Basalt. The WTR was more elevated than the YR.

AB Unit 2 seems to originate from the WTR and surrounded elevated areas. It is interpreted that the AB Unit 2 constitutes of clastic materials. During deposition of AB Unit 2 the relative sea level rose causing an enhanced accommodation space due to basin subsidence.

The deposition of AB Unit 2 indicates that both sides of the basin were at the same elevation, the basin subsided towards the SE or the area tilted towards the SE. The downlap of AB Unit 2 on reflector 2 on line 207 adjacent to line 106 (See trend on Fig. 6 and Fig. 8) indicates a compression from the NE or that the YR is divided into sections by faults or fissures.

AB Unit 3 could originate from the WTR and surrounded elevated areas. The depositional distribution is similar to AB Unit 1 and signifies that YR was not highly elevated. Compared to AB Unit 2 (Fig. 5) the accommodation space was slightly enhanced in the NE and enlarging towards the SW due to basin subsidence which indicates a relative sea level rise.

After deposition of AB Unit 3 compression commenced causing the YR and all the above deposited sedimentary units to bend upwards indicating the second ridge uplift (Fig. 6). In the NW towards the SE until line 205, erosion exposed the Top Basalt reflector indicating that this part of YR is more responsive to compression than in the SE (Fig. 8). On line 207 adjacent to the intersecting of line 106 the AB Unit 3 downlaps reflector 2 towards the SW, indicating a compression from the NE and causing a SW rotation of the YR apex. This compression may correspond to the first compressional phase described as a ridge push from the north in Late Paleocene – Early Eocene (Boldreel and Andersen, 1994). The relative sea level fell during the compression and allowed erosion of the newly uplifted areas, and thus AB Unit 3 was removed above YR.

Middle Eocene

AB Unit 4 seems to originate from the WTR and surrounded elevated areas. The AB Unit 4 has the widest distribution (Fig. 5) and during the deposition the relative sea level rose enhancing the accommodation space due to basin subsidence.

After deposition of the AB Unit 4 the Top Eocene unconformity commenced causing a pronounced relative sea level fall and indicates the third uplift of the ridges. In shallow areas truncations are found and an erosional channel is observed (Fig. 5). On lines 205-207 (Fig. 8) a precursor to the moat located adjacent to line 106 developed due to erosive sea currents. Originally AB Unit 4 was deposited above the YR and continued into the RB but later erosion removed the AB Unit 4 from line 205 towards the NW. This indicates that the first compressional phase continued until the Top Eocene or that the second compressional phase commenced from the NE.

Early Oligocene

AB Unit 5 may originate from the WTR and surrounded elevated areas. At the WTR southern flank AB Unit 5 onlaps the lower reflector except in the interval from line 206 and line 207 (Fig. 8) where AB Unit 5 onlaps reflector Top Basalt. This indicates a relative sea level rise during the deposition due to basin subsidence or sediment compaction enhancing the accommodation space.

After deposition of AB Unit 5 erosion occurred and truncated the upper boundary (Fig. 5). There are no signs of compression and thus the erosion is caused by the accommodation space being filled up.

AB Unit 6 could originate from the WTR and surrounded elevated areas. The AB Unit 6 is present to the SE of line 203 and onlaps reflector 7 before the erosional channel and the moat (Fig. 5). There are indications of a relative sea level rise towards the SE due to basin subsidence or sediment compaction during deposition of AB Unit 6.

The lack of deposition of AB Unit 6 in the NW is due to erosion caused by the Top Oligocene unconformity caused by compression that elevated the area in the NW signifying the fourth ridge uplift and a relative sea level fall. This compression indicates the third compressional phase which may correspond to the second compressional phase described as a ridge push from the north-north-west in Oligocene (Boldreel and Andersen, 1994). This implies that the ridge is divided into segments where the segment SE of line 203 experienced basin subsidence or sediment compaction.

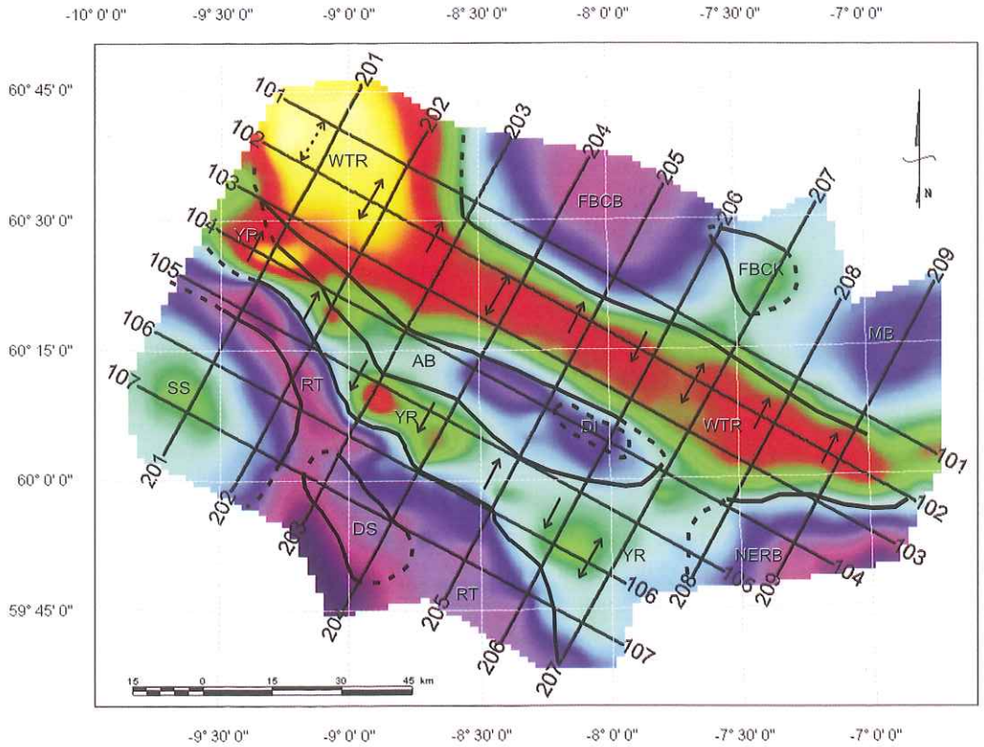

Fig. 7.
An isopach map of the interpreted Top Basalt surface to the seafloor that outlines the interpreted geological structures. Solid lines are interpreted from the YMR97 survey and dotted lines are tentative interpretations. Arrows indicate the present apex facing directions of the WTR and YR being the resultant compressional force affecting the WTRC. Abbreviations: AB, Auðhumla Basin; DIC/DS Darwin Igneous Center; DI, Drekaeyga Intrusion; FBCB, Faroe Bank Channel Basin; FBCK, Faroe Bank Channel Knoll; MB, Munkur Basin; NERB, Northeast Rockall Basin; RB, Rockall Basin; SIC/SS, Sigmundur Igneous Centre; WTR, Wyville Thomson Ridge; YR, Ymir Ridge.

Early Miocene

AB Unit 7 seems to originate from the WTR and surrounded elevated areas. The distribution of AB Unit 7 indicates that during the deposition the accommodation space enhanced more in the SE than in the NW (Fig. 5) due to basin subsidence or sediment compaction resulting in a relative sea level rise.

After deposition of AB Unit 7 the Middle Miocene unconformity commenced and the sea currents eroded the upper part of the AB Unit 7 (Fig. 5). A massive compression from the NE rotated the apex of the YR and all the above deposited units towards the SW (Fig. 6) and indicates the fifth uplift of the YR resulting in a relative sea level fall. This compression signifies the fourth compressional phase which may correspond to the third compressional phase (Boldreel and Andersen, 1994) and the second compressional phase by Andersen *et al.* (2002).

Late Miocene – Early Pliocene or Middle Pliocene – Pleistocene

AB Unit 8 may originate from the WTR and surrounded elevated areas and is deposited during a relative sea level rise due to basin subsidence.

After deposition of AB Unit 8 the Glacial Unconformity commenced and the relative sea level fell. The previously mentioned erosional channel on line 104 (Fig. 5) began to develop at the Glacial Unconformity and eroded down into reflector 6 (AB Unit 4) being the NE part of the moat located on line 203.

Pleistocene

AB Unit 9 may originate from the WTR and surrounded elevated areas and is deposited during a relative sea level rise due to basin subsidence.

Summarizing the three Sub Areas

Discussion/Conclusion

The three sub areas are connected using seismic line 206 (Fig. 6). In the text the units are to be found in Figures 3, 4 and 5.

Early Eocene

The Early Eocene comprises five units (Fig. 2): unit 1 (Top Basalt – reflector 1) located in the FBCB, unit 2 (Top Basalt – reflector 2) found in all three basins, unit 3 (between reflectors 2 - 3) present in the FBCB, unit 4 (between reflectors 2 - 4) and unit 5 (between reflectors 4 - 5) which both are found in all three basins.

The WTR started to elevate during the Early Eocene and the units deposited in the FBCB did not continue into the AB. The YR was not highly elevated and therefore the units are found in both the AB and the RB. Overall the WTRC tilted towards the SE and the ridges are segmented by faults having a NE-SW direction bearing the Caledonian trend or by fissures that connect the volcanic centres (Fig. 8). The volcanic centres, the extension of the lava flows and the transcurrent fault, which is the north western part of the Ymir/Ness Lineament, located underneath and alongside the YR controlled much of the depositional distribution and the localization of the compression. Therefore the effect of the compression is more intense in the NW of the AB and in the SE in the RB. During Early Eocene the YR started to elevate and the WTR continued to elevate due to compressional forces having a NE-SW direction. The first compression originated from the NE (during deposition of unit 1), the second from the SW (taken place during deposition of unit 2) and the third also from the NE (during deposition of unit 3, 4 and 5).

The compression from the SW may be ascribed to the seafloor spreading between Greenland and Eurasia linked at a triple junction south of Greenland (Lundin and Doré, 2005) (Fig. 1) that initiated in Paleocene (57-56 Ma Chron 24/25) (Larsen, 1988) or (c.56-53 Ma) (Saunders et al., 1997). However, the oceanic spreading between the Faroe Fracture Zone (Bott, 1985) and the Jan Mayen Fracture Zone transferring to the NW (Fig. 1) isolating the Jan Mayen microcontinent (e.g. Nunns, 1983) also had an affect on the WTRC. Many suggestions exist on the timing of the Aegir Ridge transition and judged from the internal reflector pattern outlined in this study the period from the initiation of break-up in Paleocene – Early Oligocene (Chron 24 c.54 Ma until Chron 12 c.32 Ma) when Aegir Ridge was abandoned (Lundin and Doré, 2005) is suggested. This ridge transition is manifested on the Faroe-Rockall Plateau (Boldreel and Andersen, 1993) and is the compressional force from the NE observed in the WTRC. A clockwise rotation of the WTRC is suggested by the opposed compressional directions and the different facing directions of the apex of the ridges (Fig. 7), and the strength of the affect depends on the width of the ridges. This could correspond to the first compressional phase described as a ridge push from the north in Late Paleocene – Early Eocene by Boldreel and Andersen (1994) and as the first compressional phase in the Middle Eocene by Andersen et al.

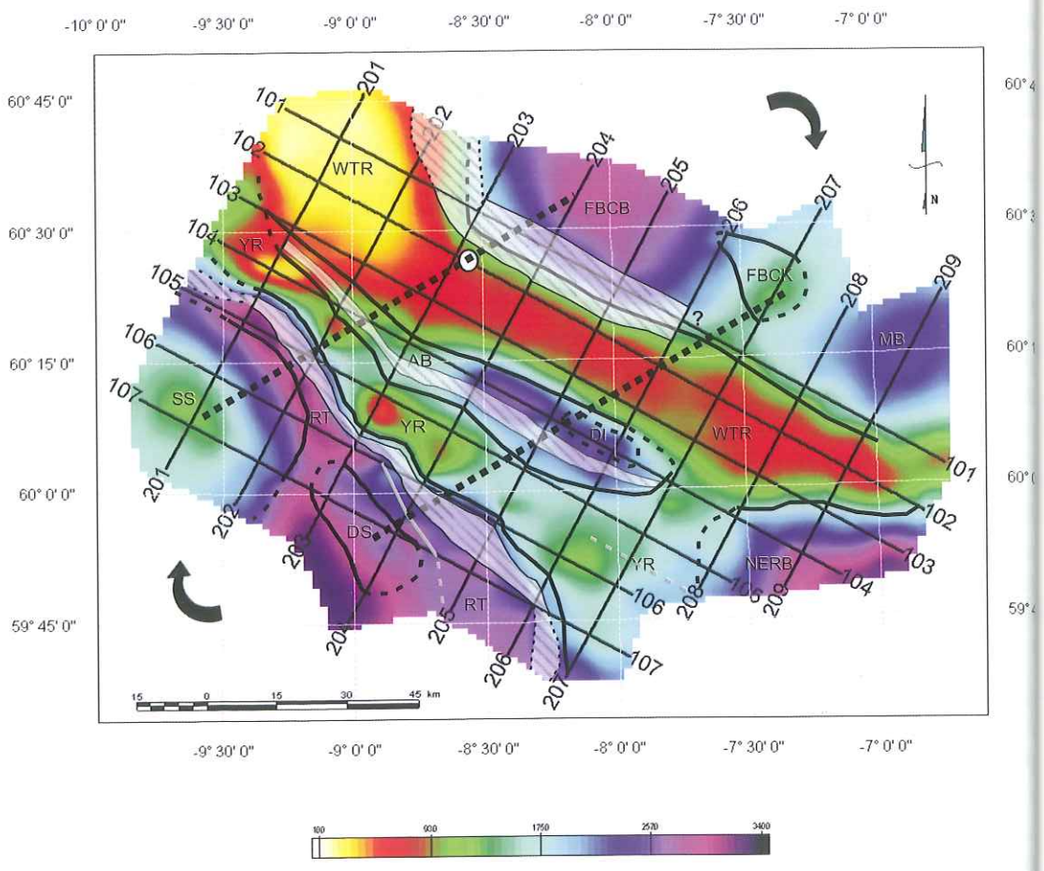

Fig. 8.
A suggested structural model of the WTRC as judged from the seismic interpretation of the seismic survey YMR97. Solid and dotted grey lines are parts of the transcurrent faults Ymir/Ness Lineament. Shaded areas show the compressional belts. Question mark relates to the shaded area in the FBCB. White dot indicates a small basin located at the Top Basalt on the WTR. Heavy dotted black lines show fissures and adjacent faults. Solid black arrows indicate clockwise rotation of the WTRC.

(2002). The Thulean Volcanic Line (Hall, 1981) (Fig. 1) located south of the WTRC, indicates a NE-SW extensional stress field (England, 1988) in the Middle Paleocene (c. 62-58 Ma) (Archer et al., 2005) that together with the mafic laccolithic located in the NE Rockall Basin could have affected the subsidence in the SE due to thermal cooling.

Overall the relative sea level rose towards the SE and enhanced the accommodation space but fell in the NW allowing erosion of the uplifted areas that removed all or parts of the units at th YR southern flank.

Middle Eocene

The Middle Eocene is comprised of one unit (Fig 2): unit 6 (between reflectors 5 - 6) deposited i all three basins and has the widest geographica distribution of all the mapped units.

The relative sea level rose during the depo sition of the unit caused by basin subsidenc that enhanced the accommodation space. Th

transcurrent fault in the RB that branches out as a listric fault in the NW direction was active.

After deposition of the unit the relative sea level fell and the Top Eocene unconformity evolved which caused a sedimentation stop and erosion of the upper boundary. This indicates that the first compressional phase continued or that the second compressional phase started from the NW. This compression may be due to the continuous spreading axis between the Arctic and the NE Atlantic in the Late Eocene (Chron 13) (Lundin and Doré, 2005) that initiated after the ocean spreading in the Labrador Sea slowed and stopped in Middle – Late Eocene (c. 50 Ma until 36 Ma Chrons 21-13) (Saunders *et al.*, 1997). Also the rotation of the Jan Mayen microcontinent manifested on the Faroe-Rockall Plateau and the WTRC contributed to the development of the Top Eocene unconformity (e.g. Johnson *et al.*, 2005 and Stoker *et al.*, 2005). These tectonic movements caused a further clockwise rotation of the WTRC.

Early Oligocene

The Early Oligocene is comprised of three units (Fig. 2): unit 7 (between reflectors 6 – 7) and unit 8 (between reflectors 7 – 8) deposited in the RB and the AB, and unit 9 (between reflectors 6 – 8) deposited in the FBCB.

The lows created at the Top Eocene unconformity became filled as the accommodation space enhanced due to basin subsidence or sediment compaction indicating a relative sea level rise. The transcurrent fault in the RB (Fig. 8) was active at the beginning of the period.

After deposition of the units the Top Oligocene unconformity commenced and the upper boundary was eroded which indicates a relative sea level fall caused by compression. The north western area of the ridges was elevated but the south eastern area subsided signifying that the ridges are segmented or that the clockwise rotation of the WTRC was reactivated (Fig. 8). In the NW of the AB and at the YR southern flank the entire unit was removed. This is caused by the third compressional phase which could correspond to the second compressional phase described as a ridge push from the north-north-west in Oligocene by Boldreel and Andersen (1994).

Early Miocene

The Early Miocene is comprised of one unit (Fig. 2): unit 10 (between reflectors 8 – 9) deposited in all three basins.

During deposition of the unit the accommodation space enhanced due to basin subsidence or sediment compaction that indicates a relative sea level rise, but in the AB the unit only exists SE of the erosional channel and the moat (Fig. 5).

After deposition of the unit the Middle Miocene unconformity commenced eroding and truncating most of the upper boundary by sea bottom currents in the AB and RB and transported the sediments as contourites and sinusoidal sediment waves (Fig. 7 and 4). This signifies the fourth compressional phase which could correspond to the third compressional phase described as a ridge push from the north-west in Middle – Late Miocene (Boldreel and Andersen, 1994) and as the second compressional phase by Andersen *et al.* (2002). This last compressional phase originating from the NW may be caused by the remnants of the structural adjustment of the rotation of the Jan Mayen microcontinent. The effect of the compressional force is that the apex of the YR and all the above deposited units turned towards the SW (Fig. 7) and indicates that the ridges are segmented and the relative sea level fell due to uplift of the ridges.

Late Miocene – Early Pliocene

The Late Miocene – Early Pliocene comprises three units (Fig. 2): unit 11 (between reflectors 9 - 10) and unit 12 (between reflectors 10 - 11) deposited in the RB, and unit 13 (between reflectors 9 - 11) deposited in the FBCB.

In the FBCB deposition took place during calm conditions, as compared to the RB, and the relative sea level was about the same as in the previous period or rose slightly enhancing the accommodation space due to basin subsidence (Fig.3). In the RB (Fig. 4) the relative sea level

rose due to basin subsidence and sea bottom currents that eroded the lower units and transported the sediments adjacent to the escarpment and flank of the YR as sinusoidal sediment waves or contourite deposits filling up the moat and lows.

After the contourite deposition the Pliocene unconformity commenced where the sea bottom currents changed their direction or strength and developed a new moat at the YR southern flank in the NW.

Middle Pliocene - Pleistocene

The Middle Pliocene – Pleistocene comprises two units (Fig. 2): unit 14 (between reflectors 9 - 12) deposited in the AB, and unit 15 (between reflectors 11 - 12) deposited in the RB and FBCB.

During deposition of the unit the relative sea level rose due to basin subsidence. In the FBCB the unit was deposited under more calm conditions than in the AB and the RB (Fig. 6).

After deposition of the unit erosion took place indicated by the Glacial Unconformity and a relative sea level fall. This signifies that the accommodation space was filled up and the onset of the glaciation. In the RB there are no indications of the Glacial Unconformity (Fig. 4), but in the AB an erosional channel developed (Fig. 5) that eroded down into the Top Eocene period being the NE part of the moat. Therefore, unit 14 (between reflectors 9 - 12) might be part of the Late Miocene – Early Pliocene period as the top of the unit has been severely eroded. Hence the Middle Pliocene – Pleistocene is not present in the AB. In the FBCB the entire upper boundary is eroded and truncated in the NW (Fig. 3).

Pleistocene

The Pleistocene is comprised of one unit (Fig. 2): unit 16 (reflector 12 – Sea Bed) deposited in all three basins. During deposition of the unit the relative sea level rose due to basin subsidence where the depositional conditions overall were more calm than in the two previously periods.

Structural Model of the WTRC

The WTRC constitute of the two NW-SE striking compressional ridges, the WTR and the YR with the intervening AB. To the NW and SE the ridges merge and at these locations the ridges have their largest width. The width of the WTR is rather consistent whereas alongside the YR the width changes (Fig. 7).

The apex of the ridges faces in different directions (Fig. 7) and this is caused by the combined effect of approximately perpendicular directed stress towards the ridges and the location of the volcanic centres thought of as being connected by two ENE/WSW trending fissures (Fig. 8). The western fissure connects the SIC and a small sediment basin on top of the WTR apex whereas the eastern fissure connects the DIC, DI and the FBCK. The fissures divide the investigated area into three parts where the NW segment had a resultant compressional direction towards the NE, the central segment towards the SW and the SE segment towards the NE (Fig. 7). Two facing directions deviate from this: in the central part of the WTR the apex faces towards NE (line 205) and in the SE the apex of the YR faces towards the SW (line 206). This local effect is caused by the width of the ridges and the location of the DI, as it is speculated that the volcanic centres absorbed and stopped much of the compressional forces and thereby locally controlled the development of the ridges. Adjacent to the fissures two NE/SW trending transfer faults that bear the Caledonian trend are interpreted (Fig. 8). In addition a transcurrent fault, which extends from the Ymir/Ness Lineament, is located underneath the south eastern part of the YR that was active until late Early Eocene. In the RB the transcurrent fault is located alongside the southern flank of YR and ends as a listric fault between the DI and the central part of the YR that was active until Early Oligocene. The WTRC tilted towards the SE due to thermal cooling of the Thulean Volcanic Line located south of the WTRC and the mafic laccolithic in the NE Rockall Basin. Four compressional phases, listed below, affected the complex and caused compressional belts alongside the flanks of the ridges and a clockwise rotation.

1. Late Paleocene – Early Eocene: the compressional force has a NE-SW direction and constitutes of three smaller compressional forces that overall resulted in a clockwise rotation of the WTRC. The first compressional force originated from the NE may be due to oceanic spreading between the Faroe Fracture Zone and the Jan Mayen Fracture Zone transferring north westwards and isolated the Jan Mayen microcontinent. This ridge transition caused the Jan Mayen microcontinent to rotate anticlockwise. The second compressional force originated from the SW may be due to the seafloor spreading between Greenland and Eurasia. The third compressional force originated from the NE is a continuation of the first compressional force due to the ridge transition that caused the anticlockwise rotation of the Jan Mayen microcontinent.
2. Late Eocene: the compressional force that originated from the NW may be due to the new continuous spreading axis between the Arctic and NE Atlantic and the rotation of the Jan Mayen microcontinent.
3. Late Oligocene: the compressional force that originated from the NW caused a reactivation of the clockwise rotation of the WTRC.
4. Middle Miocene: the compressional force originated from the NW is due to the remnants of the structural adjustment of the anticlockwise rotation of the Jan Mayen microcontinent.

Acknowledgments

Thanks are due to Fugro Geoteam for the use of the commercial 2D digital seismic survey; Landmark for issuing a software University Grant to the IGG and the Jarðfeingi for accepting this article.

References

Andersen, M. S., Sørensen, A. B., Boldreel, L. O. and Nielsen, T. 2002. Cenozoic evolution of the Faroe Platform: comparing denudation and deposition. *In*: Doré, A. G., Cartwright, J. A., Stoker, M. S., Turner, J. P. and White, N. (eds.) *Exhumation of the North Atlantic Margin: Timing, Mechanisms and Implications for Petroleum Exploration*. Special Publications Geological Society, London 196: 291-311.

Andersen, M. S., Nielsen, T., Sørensen, A. B., Boldreel, O. L. and Kuijpers, A. 2000. Cenozoic sediment distribution and tectonic movements in the Faroe region. *Global and Planetary Changes* 24: 239-259.

Archer, S. G., Bergman, S. C., Iliffe, J., Murphy, C. M. and Thornton. M. 2005. Palaeogene igneous rocks reveal new insights into the geodynamic evolution and petroleum potential of the Rockall Trough, NE Atlantic Margin. *In*: Basin Research (2005) 17: 171-201.

Boldreel, L. O. and Andersen, M. S. 1994. Tertiary development of the Faroe-Rockall Plateau based on reflection seismic data. *Bulletin of the Geological Society of Denmark* 41: 162-180.

Boldreel, L. O. and Andersen, M. S. 1993. Late Pliocene to Miocene compression in the Faeroe-Rockall area. *In*: Parker, J. R. (ed.) *Petroleum Geology of Northwest Europe: Proceedings of the 4th Conference*. Geological Society, London: 1025-1034.

Bott, M. H. P. 1985. Plate Tectonic Evolution of the Icelandic Transverse Ridge and Adjacent Regions. *Journal of Geophysical Research* 90: 9953-9960.

Cole, J. E. and Peachey, J., 1999. Evidence for pre-Cretaceous rifting in the Rockall Trough: an analysis using quantitative plate tectonic modelling. *In*: Fleet, A. J. and Boldy, S. A. R. (eds.) *Petroleum Geology of Northwest Europe: Proceedings of the 5th Conference*. Geological Society, London: 359-370.

Dean, K., McLachlan, K. and Chambers, A. 1999. Rifting and development of the Faroe-Shetland Basin. *In*: Fleet, A. J. and Boldy, S. A. R. (eds.) *Petroleum Geology of Northwest Europe: Proceedings of the 5th Conference*. Geological Society, London: 533-544.

Doré, A. G., Lundin, E. R., Jensen, L. N., Birkeland, Ø., Eliassen, P. E. and Fichler, C. 1999. Principal tectonic events in the evolution of the northwest European Atlantic margin. *In*: Fleet, A. J. and Boldy, S. A. R. (eds.) *Petroleum Geology of*

Northwest Europe: Proceedings of the 5th Conference. Geological Society, London: 41-61.

Eldholm, O. and Thiede, J. 1980. Cenozoic continental separation between Europe and Greenland. *Palaeogeography, Palaeoclimatology, Palaeoecology* 30: 243-259.

England, R. W. 1988. The early Tertiary stress regime in NW Britain: evidence from the patterns of volcanic activity. *In*: Morton, A. C. and Parson, L. M. (eds.) *Early Tertiary Volcanism and the Opening of the NE Atlantic*. Geological Society, London, Special Publications 39: 381-389.

Hall, J. M. 1981. The Thulean Volcanic Line. *In*: Kerr, J. W., Fergusson, A. J. and Machan, L. C. (eds.) *Geology of the North Atlantic borderlands*. Canadian Society of Petroleum Geologists, Memoirs 7: 231-244.

Hinz, K., Eldholm. O., Block, M. and Skogseid, J. 1993. Evolution of the North Atlantic volcanic continental margins. *Petroleum Geology of Northwest Europe: Proceedings of the 4th Conference*: 901-913.

Johnson, H., Ritchie, J. D., Hitchen, K., Mcinroy, D. B. and Kimbell, G. S. 2005. Aspects of the Cenozoic deformational history. *In*: Doré, A. G. and Vining, B. A. (eds.) *Petroleum Geology: North-West Europe and Global Perspectives—Proceedings of the 6th Petroleum Geology Conference*. Geological Society, London: 993-1007.

Keser Neish, J. and Ziska, H. 2005. Structure of the Faroe Bank Channel Basin, offshore Faroe Islands. *In*: Doré, A. G. and Vining, B. A. (eds.) *Petroleum Geology: North-West Europe and Global Perspectives—Proceedings of the 6th Petroleum Geology Conference*. Geological Society, London: 873-885.

Kimbell, G. S., Ritchie, J. D., Johnson, H. and Gatliff, R. W. 2005. Controls on the structure and evolution of the NE Atlantic margin revealed by regional potential field imaging and 3D modelling. *In*: Doré, A. G. and Vining, B. A. (eds.) *Petroleum Geology: North-West Europe and Global Perspectives—Proceedings of the 6th Petroleum Geology Conference*. Geological Society, London: 933-945.

Larsen, H. C. 1988. A multiple and propagating rift model for the NE Atlantic. *In:* Parson, L. M. and Morton, A. C. (eds.) *Early Tertiary Volcanism and the Opening of the NE Atlantic*. Geological Society, London. Special Publication 39: 157-158.

Lundin, E. R. and Doré, A. G. 2005. NE Atlantic break-up: a re-examination of the Iceland mantle plume model and the Atlantic–Arctic linkage. *In*: Doré, A. G. and Vining, B. A. (eds.) *Petroleum Geology: North-West Europe and Global Perspectives—Proceedings of the 6th Petroleum Geology Conference*. Geological Society, London: 739-754.

Nunns, A. G. 1983. Plate tectonic evolution of the Greenland–Scotland Ridge and surrounding regions. *In*: Bott, M. H. P., Saxov, S., Talwani, M. and Thiede, J. (eds.) *Structure and development of the Greenland–Scotland Ridge: new methods and concepts*. Plenum Press, New York: 11-30.

Passey, S. R. and Bell, B. R. 2007. Morphologies and emplacement mechanisms of the lava flows of the Faroe Islands Basalt Group, Faroe Islands, NE Atlantic Ocean. *Bulletin of Volcanology* 70: 139-156.

Posamentier, H. W. and Allen, G. P. 1999. Siliciclastic Sequence Stratigraphy – Concepts and Applications. SEMP *Concepts in Sedimentology and Paleontology* No. 7. Tulsa, Oklahoma, U.S.A.

Roberts, D. G., Thompson, M., Mitchener, B., Hossack, J., Carmichael, S. and Bjørnseth, H.-M. 1999. Palaeozoic to Tertiary rift and basin dynamics: mid-Norway to the Bay of Biscay – a context for hydrocarbon prospectivity in the deepwater frontier. *In*: Fleet, A. J. and Boldy, S.A.R. (eds.) *Petroleum Geology of Northwest Europe: Proceedings of the 5th Conference*. Geological Society, London: 7-40.

Saunders, A. D., Fitton, J. G., Kerr, A. C., Norry, M. J. and Kent, R.W. 1997. The North Atlantic Igneous Province. *In*: Mahoney, J. J. and Coffin, M. L. (eds.) *Large Igneous Provinces*. Geophysical Monograph Series, American Geophysical Union, Washington DC.

Smith, L. K., White, R. S., Kusznir, N. J. and iSIMM TEAM. 2005. Structure of the Hatton Basin and adjacent continental margin. *In*: Doré, A. G. and Vining, B. A. (eds.) *Petroleum Geology: North-West Europe and Global Perspectives—Proceedings of the 6th Petroleum Geology Conference*. Geological Society, London: 947-956.

Smith, K., Whitley, P., Kimbell, G. S., Kubala, M and Johnson, H. 2009. Enhancing the prospectivity of the Wyville Thomson Ridge. *In:* Varming and Ziska (eds.) *Faroe Islands Exploration Conference: Proceedings of the 2nd Conference*. Annales

Societatis Scientiarum Færoensis, Supplementum 50, Tórshavn: 286-302.

Stoker, M. S., Praeg, D., Shannon, P.M., Hjelstuen, B. O., Laberg, J. S., Nielsen, T., Van Weering, T. C. E., Sejrup, H. P. and Evans, D. 2005. Neogene evolution of the Atlantic continental margin of NW Europe (Lofoten Islands to SW Ireland): anything but passive. *In*: Doré, A. G. and Vining, B. A. (eds.) *Petroleum Geology: North-West Europe and Global Perspectives—Proceedings of the 6th Petroleum Geology Conference*. Geological Society, London: 1057-1076.

STRATAGEM Partners. 2002. *The Neogene stratigraphy of the glaciated European margin from Lofoten to Porcupine*. Stoker, M S (compiler). A product of the EC-supported STRATAGEM project.

Sørensen, A. B., 2003. Cenozoic basin development and stratigraphy of the Faroese area. Petroleum Geoscience, **9**, 189-207.

Talwani, M. and Eldholm, O. 1977. Evolution of the Norwegian-Greenland Sea. *Geological Society of America Bulletin* 88: 969-999.

Tate, M. P., Dodd, C. D. and Grant, N. T. 1999. The Northeast Rockall Basin and its significance in the evolution of the Rockall–Faroes/East Greenland rift system. *In*: Fleet, A. J. and Boldy, S. A. R. (eds.) *Petroleum Geology of Northwest Europe: Proceedings of the 5th Conference*. Geological Society, London: 391-406.

Waagstein, R. 1988. Structure, composition and age of the Faroe basalt plateau. In: Parson, L. M. and Morton, A. C. (eds.) *Early Tertiary Volcanism and the Opening of the NE Atlantic*. Geological Society, London. Special Publication 39: 225-238.

White, R. S., Spence, G. D., Fowler, S. R., McKenzie, D. P., Westbrook, G. K. and Bowen, N. 1987. Magmatism at rifted continental margins. *Nature* 330: 439-444.

Ziegler, P. A. 1987. Compressional intra-plate deformations in the Alpine foreland – an introduction. *Tectonophysics* 137: 1-5.

List of Figures:

Figure 1: Geographical map of the North Atlantic including structural features in the region and the seismic survey YMR97 interpreted in this study.

Figure 2: Stratigraphic correlation diagram of successions and their bounding unconformities or conformable reflectors in this study correlated to previous authors work.

Figure 3: WNW-ESE seismic line 101 located in the FBCB.

Figure 4: WNW-ESE seismic line 107 located in the RB.

Figure 5: WNW-ESE seismic line 104 located in the AB.

Figure 6: NNE-SSW seismic line 206 connecting the FBCB, AB and RB.

Figure 7: Geological structures outlined and the apex facing directions of the WTR and the YR.

Figure 8: Structural model of the WTRC.

List of Abbreviations

Auðhumla Basin = AB

Bill Bailey Bank = BBB

British Volcanic Province = BVP *Continent-Ocean Boundary = COB*

Darwin Igneous Centre = DIC Drekaeyga Intrusion = DI

Faroe Bank Channel Basin = FBCB Faroe Bank Channel Knoll = FBCK

Faroe Shetland Basin = FSB *Greenland – Faroes Ridge = GFR*

Large Igneous Province = LIP Munkur Basin = MB

Munkagrunnur Ridge = MR North Atlantic Igneous Province = NAIP

Northeast Rockall Basin = NERB *Norwegian Sea Deep Water = NSDW*

Rockall Basin = RB Seaward Dipping Reflectors = SDR

Sigmundur Igneous Centre = SIC Wyville Thomson Ridge = WTR

Wyville Thomson Ridge Complex =WTRC Ymir Ridge = YR